Component Dynamics in Miscible Polymer Blends: A Two-Dimensional Deuteron NMR Investigation

G.-C. Chung and J. A. Kornfield*

Division of Chemistry and Chemical Engineering, California Institute of Technology, Pasadena, California 91125

S. D. Smith

Procter & Gamble, Cincinnati, Ohio 45239

Received August 9, 1993; Revised Manuscript Received November 22, 1993®

ABSTRACT: The dynamics of individual components in 1,4-polyisoprene/poly(vinylethylene) miscible blends are studied using two-dimensional deuteron exchange NMR. The rate of the backbone reorientation process near the glass transition is quantitatively determined for each species in a miscible blend as a function of temperature. We demonstrate that the broad glass transition arises both from a wide distribution of segmental motional rates for each species and from intrinsic differences in the motional rate between the two species. In addition, the temperature dependence of their motional rates in the blend DSC glass transition region suggests that the two components undergo distinct effective glass transitions, which is consistent with previously observed thermorheologically complex behavior. The origins of dynamic heterogeneity are examined further by comparing the experimental results with a simple model calculation that takes into account the effect of composition variations in an ideal miscible blend. This comparison suggests that the observed dynamic heterogeneities can be explained only by including two distinct contributions: local composition variations in the blend *and* intrinsic differences in chain mobilities.

1. Introduction

Polymer blends are of great practical interest because a range of useful materials can be produced by blending existing polymers. Given that most blends are only partially miscible, the challenge of predicting the properties of polymer blends raises scientific questions regarding the development of their phase-separated morphology, control of interfacial properties, and dependence of the properties of each phase on composition and temperature.[1] In this study, we focus on the effect of temperature and composition on the chain dynamics that control the viscoelastic and transport properties of each phase. We use a miscible blend as a model system.[2] In addition to the practical value of clarifying the contribution of each phase to blend properties, the study of miscible blends addresses persistent fundamental questions regarding chain dynamics in homopolymers as well: For given neighboring chains, how do the dynamics of a polymer depend on its particular structure? For a given chemical structure, how do chain dynamics depend on the composition of neighboring chains?

Indeed miscible blends exhibit viscoelastic behaviors that suggest that the individual species retain distinct motional characteristics and that their mobilities are sensitive to the composition of neighboring chains. The most pronounced examples are an anomalously broad glass transition[3-7] and failure of time–temperature superposition.[7,8] Related to the molecular origins of these phenomena, dynamic heterogeneities in miscible blends have been observed recently both at a segmental[9,10] and a macromolecular level.[11-13] For example, infrared dichroism measurements have shown that when a miscible blend is deformed, each component in it can exhibit different degrees of orientation and relaxation dynamics.[11,13] Further, ^{13}C NMR line-width and relaxation time measurements have indicated distinct mobilities of each component at a segmental level.[9,10] Though these observations clearly demonstrate the existence of dynamic heterogeneity in miscible blends, little quantitative information is available regarding the dynamics of each component and their relationship to the macroscopic properties of blends.

For example, in explaining the broad glass transition, some authors emphasize the role of broadening of the dynamics of both components by heterogeneity in local composition,[3,4,14] while others emphasize the intrinsic differences in mobility of the two components.[9] Similarly, the failure of time–temperature superposition is attributed by some to the effect of local composition variations[8] and by others to the distinct temperature dependence of the dynamics of each species.[7] Few authors have considered both effects simultaneously,[15,16] and indeed no previous experimental studies have examined the effect of blending both on the distribution of motional rates of both species and on their mean motional rates.

Here we provide quantitative experimental measurements of the dynamics of each component in a blend. We use these results to assess the roles of local composition variations and intrinsic differences in mobility in producing heterogeneous dynamics in polymer blends. We focus on local segmental motions that have been associated with the glass transition. Therefore, the results pertain directly to understanding the origins of the broad glass transition of miscible blends. Knowledge of the local segmental motion of each component also represents a first step toward understanding the failure of time–temperature superposition, which requires further knowledge of the way that heterogeneity in local segmental motion propagates out to the larger molecular scale represented by a Rouse segment.

To quantitatively characterize the dynamics of each species in a blend, we use both selective isotopic labeling and appropriate spectroscopic techniques. Local segmental dynamics are measured using two-dimensional deuteron exchange NMR (2D ^2H NMR). To determine the relationship between local chain motions and the larger length scale relaxations that control melt rheology, we coordinate this study with a rheooptical investigation of the contribution of each species to blend viscoelasticity.[17]

® Abstract published in *Advance ACS Abstracts*, January 15, 1994.

0024-9297/94/2227-0964$04.50/0

This experimental approach gives several distinct advantages over previous studies:[1-11] (1) the dynamics of each component are clearly resolved by both 2D ^2H NMR and dynamic IR dichroism, (2) the rate of segmental reorientation of the backbone is quantitatively determined using 2D ^2H NMR, (3) the width of the distribution of segmental mobilities is estimated using 2D ^2H NMR, and (4) the overall chain conformational relaxation dynamics of each component are quantitatively characterized using simultaneous mechanical and optical measurements.

In this work, blends of poly(vinylethylene) (PVE) (a.k.a. 1,2-polybutadiene) and 1,4-polyisoprene (PI) are used as model systems. This pair is ideal for our study since it has been shown to be miscible in all proportions, yet has very weak interaction.[18-20] Although, on the basis of inspection of their chemical structure, one would expect these polymers to experience unfavorable dispersion interactions, recent SANS experiments have shown that PVE/PI blends can be described by an interaction parameter, χ, that is small but negative at all accessible temperatures.[18] This indication that the blend is completely miscible without specific interaction is consistent with numerous previous studies.[19-24] Furthermore, although the DSC glass transition of this blend is broad, the DSC traces of both blends and block copolymers of a given overall composition are the same.[6,7,22,25] The identical DSC traces of blends and block copolymers suggest that dynamic heterogeneity in this system is *not* due to concentration fluctuations associated with incipient phase separation, since these would be suppressed in block copolymers relative to blends. The absence of such an effect is in accord with $\chi < 0$.[18] Instead, dynamic heterogeneity could trace back to local variations in compositions that are purely statistical. Here, the PI/PVE blend provides a model system ($\chi \simeq 0$) in which these statistics can be treated by assuming random segmental mixing.

In the next section, we describe our experimental approach. We then present the correlation time of segmental motion as a function of temperature for the two pure components and each species in a 50/50 blend. The results are then discussed in light of the questions raised above and compared with other studies and with a simple model of the local segmental dynamics. We conclude with a brief summary of our findings.

2. Experimental Section

2.1. Materials. Four polymers are used in these experiments: hydrogenous and deutero 1,4-polyisoprene (PI and dPI) and hydrogenous and deutero poly(vinylethylene) (PVE and dPVE). All polymers are prepared by anionic synthesis and have narrow molecular weight distributions. The glass transition temperature of each species and their miscibility are known to depend strongly on the microstructure of PI and PVE.[9,23,26] The microstructures of PI and PVE are determined by ^{13}C NMR. Room-temperature ^{13}C NMR spectra are obtained from 15% (w/v) $CDCl_3$ solutions of PI and PVE using a GE QE-300 spectrometer. Molecular weight distributions of normal and deutero PI and PVE are determined with respect to polyisoprene standards by gel-permeation chromatography (Waters ALC-GPC), operated at 60 °C with reagent-grade toluene. The ^{13}C NMR results indicate that microstructures of the matching pair of polymers are the same within experimental uncertainties (Table 1). The molecular weights of all polymers are large enough that the glass transition behavior and the local segmental dynamics studied here should not be sensitive to the small difference in molecular weight between normal and labeled chains.

Results are presented for a pair of 50/50 PI/PVE blends, one dPVE/PI and the other PVE/dPI. The blends are prepared by mixing 3 wt % toluene solutions of each component and slowly casting on a teflon film, and then drying at room temperature first under a hood and further under vacuum for more than a week. The blend films are clear and free of bubbles, suggesting that the film is homogeneous and completely dried. No antioxidant is added to the blends to avoid possible effects on the local dynamics and T_g. The blend samples are subsequently sealed off under air in NMR sample tubes and kept in the freezer to retard oxidation.

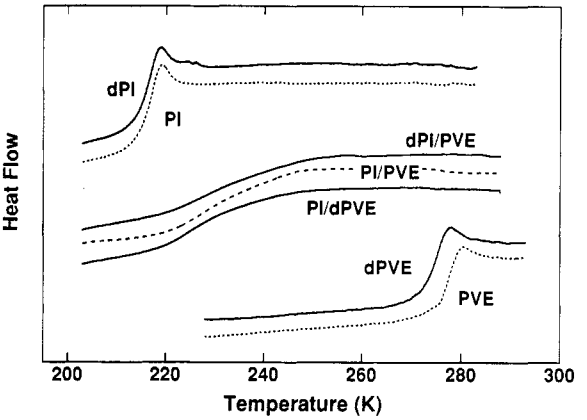

Figure 1. DSC traces for the four homopolymers (PVE, dPVE, PI, and dPI) and three 50/50 PVE/PI blends (PVE/dPI, dPVE/PI, and PVE/PI).

Table 1. PI and PVE Characterization Results

sample	$M_n \times 10^{-3}$	M_w/M_n	microstructure (%) cis-1,4	trans-1,4	3,4	T_g (K)
PI	108	1.07	78.5 ± 0.5	16.0 ± 1.0	6 ± 1.0	215
dPI	110	1.45	78 ± 1.5	15 ± 1.5	7 ± 2	215

sample	$M_n \times 10^{-3}$	M_w/M_n	microstructure (%) 1,2	1,4	T_g (K)
PVE	83	1.06	94 ± 2	6 ± 2	276
dPVE	69	1.36	93 ± 2	7 ± 2	274

The glass transitions of the blends and pure components are characterized by differential scanning calorimetry (DSC) (Figure 1). The DSC traces were recorded for the specimens (ca. 25 mg) between 190 and 290 K at a heating rate of 10 K/min using a Perkin-Elmer system DSC-7. The pair of PI's have essentially the same T_g, while T_g of dPVE is about 2 K lower than the normal PVE, probably due to a small difference in their microstructure.[26,27] This also affects the glass transition behavior of the PI/dPVE blends, with the inception of its increase in heat capacity being slightly steeper than that of the other two 50/50 blends. Concerning possible crystallization of PI, the present polymers are atactic and do not crystallize.[28]

2.2. Two-Dimensional Deuteron Exchange NMR. The segmental reorientation dynamics of polymers are studied near the glass transition using 2D ^2H exchange NMR.[29,30] The essence of this method is that it reveals the type and rate of segmental reorientation by correlating the deuteron resonance frequency before and after a controlled time period, t_m, called the mixing time.[29,30] The direct relationship between the segmental reorientation dynamics and the change in the deuteron magnetic resonance frequency arises from the fact that the resonance frequency (ω) depends directly on the orientation angle (θ) of the C–^2H bond with respect to the main magnetic field of the spectrometer. For the C–^2H bonds in dPI and dPVE, the electric field gradient at the deterium nucleus is essentially uniaxial about the axis of the C–^2H bond. Therefore, the orientation dependence of the resonance frequency is approximately given by

$$\Delta\omega(\theta) = \frac{\delta}{2}[3\cos^2(\theta) - 1)] \quad (1)$$

where $\Delta\omega$ is the shift of the resonance frequency from the deuteron Larmor frequency ω_0 and δ specifies the strength of the electric

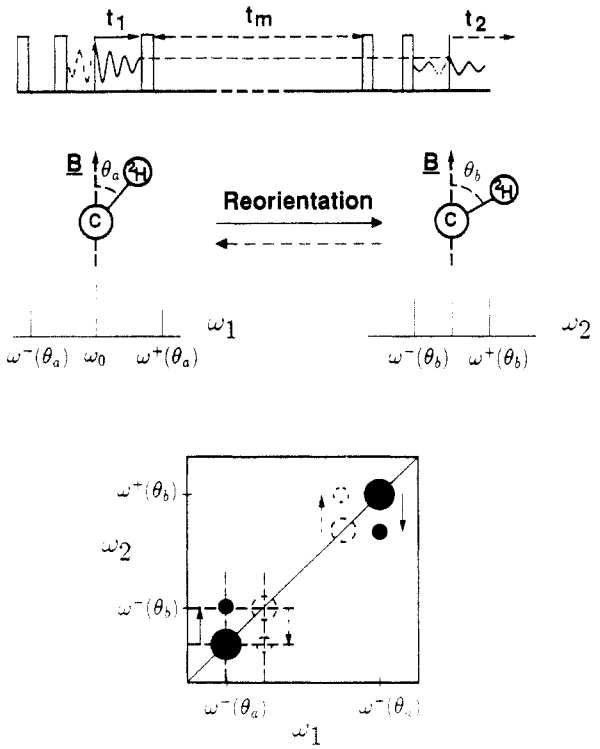

Figure 2. Scheme of the five-pulse 2D ^{2}H exchange NMR sequence. First, three radio-frequency pulses before the mixing time prepare the magnetization, the amplitude of which is sinusoidally modulated with a frequency that corresponds to the initial orientation, *i.e.*, $\omega_i^{\pm}t_1$. The last two pulses after the mixing time prepare a signal that has an initial amplitude sinusoidally modulated with $\omega_i^{\pm}t_1$ and that oscillates with a frequency that corresponds to the final orientation, *i.e.*, $\omega_f^{\pm}t_2$. The spectrum is obtained by taking the two-dimensional Fourier transform. Deuterons on bonds whose initial and final orientation angles are the same (*i.e.*, $\theta_i = \theta_f$) contribute to the intensity along the diagonal of the spectrum (for example, the large black and dashed peaks correspond to deuterons on bonds oriented at θ_a and θ_b, respectively, both at the beginning and end of the mixing time). The off-diagonal peaks in the spectrum result from orientational exchange occurring in the mixing time t_m ($\theta_i = \theta_a \rightarrow \theta_f = \theta_b$ corresponds to the small black peaks, and $\theta_i = \theta_b \rightarrow \theta_f = \theta_a$ corresponds to the small dashed peaks). See text for further discussion.

quadrupole coupling.[31] Since the deuteron is a spin $I = 1$ nucleus, two resonance lines at frequencies, $\omega^{\pm} = \omega_0 \pm \Delta\omega(\theta)$, are associated with a given C–^{2}H bond orientation.

In a one-dimensional spectrum, the relationship between ω and θ allows one to analyze the orientation distribution of C–^{2}H bonds. To gain information on molecular motions, it is useful to quantify the change in resonance frequency that occurs during a controlled interval of time. To achieve this, we use the five-pulse 2D ^{2}H exchange NMR experiment illustrated in Figure 2.[32] The spectra are acquired in the time domain, with an intensity that oscillates with the time interval t_1 as dictated by the initial orientation of the C–^{2}H bonds in the system and oscillates with the time t_2 as dictated by their final orientation after the mixing time t_m. The contributions due to just two orientations are shown in the schematic diagram. The mixing time t_m is held fixed for each 2D spectrum. If t_m is short compared to the correlation time for segmental motion, τ_c, very few C–^{2}H bonds undergo reorientation during t_m. Therefore, the spectrum will be confined to the diagonal; the initial and final resonance frequencies $\omega^{\pm}(\theta_i)$ and $\omega^{\pm}(\theta_f)$ of each ^{2}H are the same since $\theta_i = \theta_f$. If t_m is on the order of τ_c or longer, a significant fraction of C–^{2}H bonds undergo reorientation during t_m.[33] Deuterons on a C–^{2}H bond that is initially oriented at $\theta_i = \theta_a$ but has a final orientation $\theta_f = \theta_b$ contribute to the off-diagonal intensity at positions $(\omega_1, \omega_2) = (\omega^{\pm}(\theta_a), \omega^{\pm}(\theta_b))$, as shown in Figure 2. By microscopic reversibility, as many bonds reorient from $\theta_b \Rightarrow \theta_a$ as from $\theta_a \Rightarrow \theta_b$. Thus, the spectrum is symmetric about the diagonal.

In amorphous or unaligned crystalline polymers, the overall orientation distribution is isotropic, leading to a Pake pattern along the diagonal. The profile of the off-diagonal intensity shows both the type and the extent of reorientation during a particular mixing time.[29] With increasing mixing time, the spectra capture the reorientation of progressively slower-moving populations in the overall distribution of τ_c, which may have appeared rigid (diagonal intensity) at smaller t_m. Therefore, the evolution of the two-dimensional spectrum over a range of t_m reveals the distribution of rates of reorientation.

All 2D spectra are recorded using a Bruker MSL 200 spectrometer, equipped with a VT1000 temperature controller unit. A slightly modified Bruker broad-band wide-line probe with a 7.5-mm coil is used. The 90° pulse length is 3.0 μs, and a digitization rate of 2.8–3.2 μs is used to capture the complete range of the spectra along both the ω_1 and ω_2 dimensions. The repetition time is varied from 300 to 700 ms to obtain sufficiently relaxed spectra. Reasonable signal to noise is achieved with ~128 scans at the smallest mixing time and up to 960 scans at the largest mixing time. The typical data size is 256 complex points along t_2 and 60 points along t_1. At each temperature, spectra are taken at three or more mixing times, from 0.5 to 400 ms, to probe the evolution of the reorientation distribution over almost 3 decades in time. The temperature is controlled so that it remains within ±0.5 K of the set point for a set of mixing times.[35]

The shapes of the present spectra indicate that the C–^{2}H bond reorientation dynamics can be modeled as isotropic rotational diffusion of C–^{2}H bonds, as has been observed in other amorphous polymers.[34,36–38] Therefore, we fit the experimental spectra by calculating the 2D spectra arising from isotropic rotational diffusion. The mean correlation time for this process is inversely related to the effective rotational diffusivity D by $\tau_c = 1/6D$.[39] To arrive at a good fit, we first seek the value of τ_c that yields the best fit of the spectra over the range of mixing times. The qualitative shape of the evolution of the 2D spectra with t_m can be described by a single correlation time. The quantitative agreement, however, improves significantly by introducing a distribution of correlation times. The simple log Gaussian distribution of correlation times is found to fit the experimental spectra successfully:

$$P(\ln \tau_c) = \frac{\exp[-(\ln \tau_c - \ln \tau_{c_0})^2/2\sigma_{\ln}^2]}{(2\pi\sigma_{\ln}^2)^{1/2}} \qquad (2)$$

where $\tau_{c_0} = \exp\langle \ln \tau_c \rangle$ is the log mean correlation time and $\sigma_{\ln}$ is the log mean standard deviation.[36] The width of the correlation time distribution in decades is $\sigma = \sigma_{\ln}/\ln(10)$. Other types of correlation time distributions may be equally justifiable. We have compared the quality of fit obtained with the log Gaussian distribution to the asymmetric log Gaussian that has been used by others to mimic the asymmetry of a stretched exponential distribution.[36,40] We find that an asymmetric distribution does not improve the fit significantly, as was noticed previously.[36] Furthermore, the mean and the full width of the distribution obtained using the asymmetric distribution are consistent with those determined using the simpler log Gaussian distribution.

The procedure we use to determine τ_{c_0} and σ begins by finding the value of τ_{c_0} that produces the best fit for all t_m with σ constrained to be small, typically 1 decade. If this fit shows systematic deviations that indicate the presence of significantly faster and slower processes, the width of the distribution is increased by a half decade, and τ_{c_0} is optimized again. This is repeated until the fit can no longer be improved by increasing σ. Since the range of t_m only spans up to 3 decades, it is not possible to accurately determine σ when it exceeds 3. The fit is quite sensitive to τ_{c_0}, so uncertainties in this parameter are relatively small (less than a factor of 2).

3. Results

The 2D ^{2}H NMR spectra of the pair of 50/50 blends of PI and PVE directly show that the two species have very different mobilities (Figure 3). At this blend composition and temperature (50/50 and 237 K), there is more reorientation of PI in 5 ms than of PVE in 200 ms. In

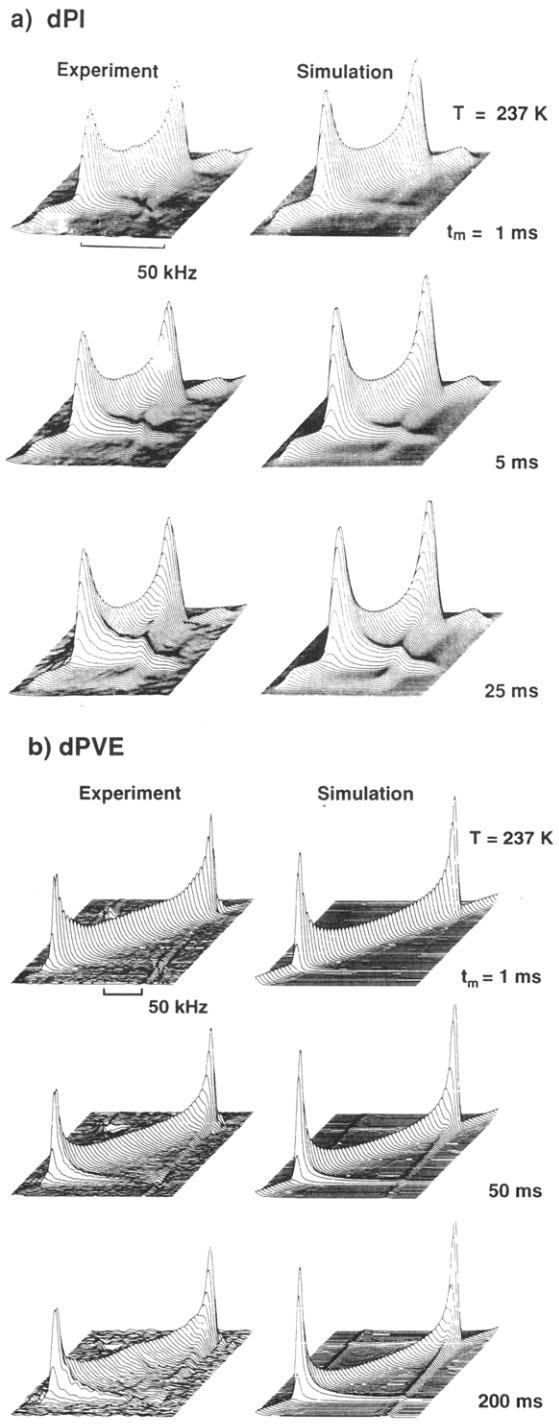

Figure 3. 2D ^{2}H exchange NMR spectra obtained at 237 K (−36 °C) for each component in the matching pair of 50/50 blends. (a) Experimental and simulated 2D ^{2}H exchange NMR spectra obtained with mixing times of 1, 5, and 25 ms for dPI in a 50/50 dPI/PVE blend. From the fit, we obtain a mean correlation time τ_{c_0} = 0.025 s and a width of the distribution σ = 3 decades. (b) Experimental and simulated 2D ^{2}H exchange NMR spectra obtained with mixing times of 1, 50, and 200 ms for dPVE in a 50/50 PI/dPVE blend. From the fit, we obtain τ_{c_0} = 0.5 s and σ = 3 decades. The width of the correlation time distribution is the same, while the mean correlation times differ by more than 1 decade.

addition, when compared to the spectra of pure components, the development of the off-diagonal intensities as a function of t_m is relatively gradual. This indicates that the distributions of the correlation time are broader for components in the blend than for the pure components.

The mean and the width of the correlation time distribution (τ_{c_0} and σ) are determined by fitting the series

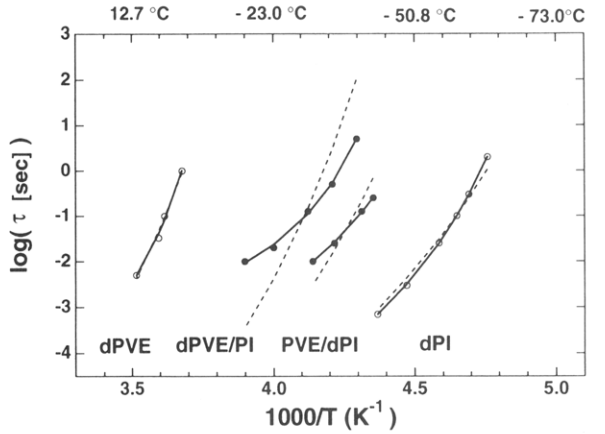

Figure 4. Log mean correlation times as a function of temperature $\tau_{c_0}(T)$. The dashed lines are obtained by using the WLF parameters C_1^g and C_2^g estimated by mechanical measurement well above T_g.[7] The solid curves are obtained by restricted WLF fits, constraining the T_g alone for pure PI and constraining $\tau_g \equiv \tau_{c_0}(T_g) = 0.32$ s for both species in the blend. The WLF parameters used here are summarized in Table 2.

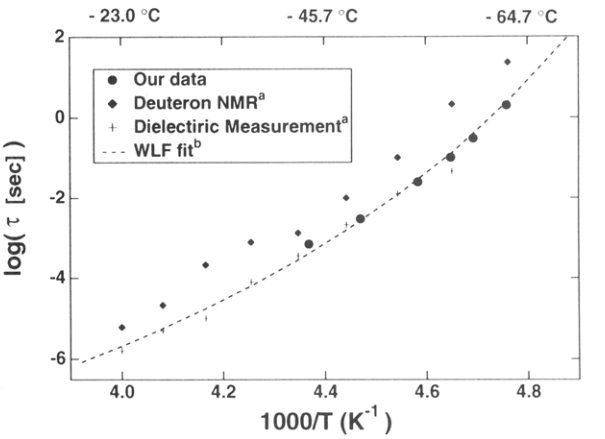

Figure 5. The mean correlation times for PI are compared with previous deuteron NMR and dielectric measurements.[36] [a]Data taken from Schaefer *et al.*[36] Their NMR data were presented based on the Bruker temperature reading; when these are shifted 5 K, all three sets of data fall on a single curve.[35] [b]The WLF fit is obtained by using the DSC T_g and C_1^g and C_2^g obtained by mechanical measurement.[7]

of experimental spectra at each temperature with calculated spectra (Figure 3). The simple log Gaussian distribution of correlation times is found to fit the experimental spectra successfully. Even for the components in the blend, no systematic deviation from this unimodal distribution is observed. This is in contrast to observations made regarding 2D ^{13}C NMR spectra of poly(2,6-dimethylphenylene oxide) (PXE) in polystyrene (PS)/PXE blends.[16]

The mean correlation times of segmental reorientation of the two homopolymers and each component in a 50/50 blend are shown in Figure 4. To check the validity of our results, we compare them with previous studies. Direct comparison is possible only for the PI homopolymer. The values of $\tau_{c_0}(T)$ for pure PI agree well with the previous 2D ^{2}H NMR and dielectric relaxation measurements (Figure 5).[36] The agreement would be nearly perfect if the previous 2D ^{2}H NMR data were shifted by 5 K.[35] The temperature dependence of τ_{c_0} for each pure component is consistent with the WLF behavior established by mechanical measurements (dashed curves through the homopolymer data in Figure 4). This is in agreement with the previous 2D ^{2}H NMR studies on a number of amorphous homopolymers.[34,36–38]

Table 2. Best Fit WLF Parameters for the Mean Correlation Time of PI and PVE in a 50/50 Blend and for Homopolymers

exptl method	sample	species	C_1^g	C_2^g	T_g	log (τ_g)
mechanical measurement[a]	homopolymer	PVE	11.4	56	275	−0.73
		PI	11.8	52.9	210	0.05
	50/50 blend	PVE	11.8	55	245	−1.4
		PI	11.8	55	233	−0.94
2D ^{2}H exchange NMR[b]	homopolymer	dPVE	6.3	26.9	274	−0.55[c]
		dPI	7.4	33	215	−0.98[c]
	50/50 blend	dPVE	3.8	25.9	239	−0.5[d]
		dPI	5.4	32.2	229	−0.5[e]

[a] Values taken from Roovers and Toporowski,[7] with log(τ_g)'s adjusted to minimize the deviation between the WLF fit and the observed mean correlation time. Dashed curves on Figure 4. [b] Solid curves on Figure 4. [c] In the fit, we used the T_g's measured by DSC for our samples. [d] log(τ_c) at T_g is constrained to be −0.5, which is the approximate value at the DSC T_g for both pure components. An unconstrained fit reaches the minimum χ^2 error for parameters 3.9, 25.2, 238.1, and −0.38. [e] log(τ_c) is constrained to be −0.5, as above.

In a 50/50 blend, the two species exhibit not only quite different mobilities at a given temperature but also distinct temperature dependencies. Whereas the segmental dynamics of homopolymers vary with temperature in accord with the WLF dependence of homopolymer viscoelasticity, this is not the case for the segmental dynamics of each species in blends. Roovers and Toporowski have inferred the temperature dependence of the relaxation of each species in PI/PVE blends using viscoelastic data (Table 2).[7] Their results for PI and PVE in a 50/50 blend are compared to τ_{c_0} for each species in Figure 4 (dashed curves through the blend data). In contrast to the homopolymers, the agreement is not good. The solid curves show the results of WLF fits to the data for each species in the 50/50 blends (parameters given in Table 2).

To relate the change in segmental mobility with temperature to the DSC glass transition, we note that the DSC T_g, obtained at a heating rate of 10 K/min, corresponds to the temperature at which τ_{c_0} for the homopolymer is between 0.1 and 1 s for both PI and PVE.[41] Analogous to the results for pure components, we can define the "effective glass transition temperature", T_g*, of each species in the blend as the temperature at which the mean correlation time of each component reaches approximately 0.32 s, *i.e.*, the middle of the range of correlation times at which the homopolymers undergo the DSC glass transition. Consistent with the observations for pure components, the temperatures at which the mean correlation times of each species in a blend become 0.32 s fall well within the DSC glass transition region (cf. Figure 1). However, the temperatures where the individual components reach this rate of motion are well separated. It is estimated that T_g* of PI is about 10 K lower than that of PVE, which is in reasonable agreement with the 15 K difference estimated by ^{13}C NMR.[9] The discrepancy between the two values may be due in part to the somewhat lower T_g of our dPVE relative to more ideal PVE (≥97% 1,2 units), which could reduce the difference in T_g* between the labeled species (dPI and dPVE) observed by ^{2}H NMR.

The width of the distribution, σ, is also determined as a function of temperature for both components in the blends and for the two pure components, presented as vertical bars in Figure 6. As the temperature decreases, σ gradually increases. This is observed even for the pure components in accord with previous observations for PI and other homopolymers.[36] In homopolymers, this trend is attributed to the heterogeneity gradually frozen in near

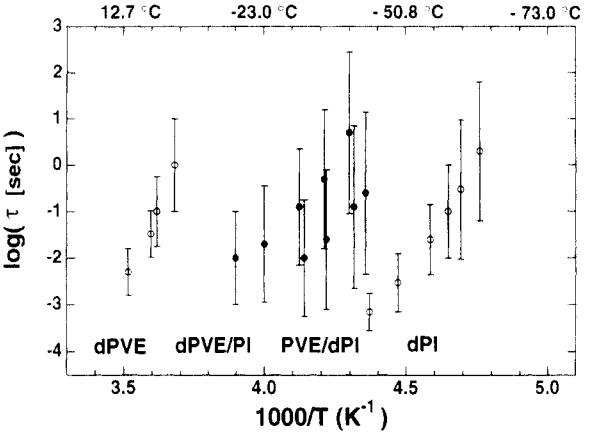

Figure 6. Width of the correlation time distribution represented by vertical bars that span ±σ. The circles show the mean correlation times of Figure 4 for reference.

the glass transition.[36] The increase in σ with decreasing T is observed for the components in the blends as well. However, the components in the blends have much greater σ than the pure components when compared at temperatures corresponding to the same mean correlation times.

For this particular pair of polymers, the distribution widths of the two pure components are comparable at temperatures corresponding to the same mean correlation times. In contrast, the two species in the blend exhibit quite similar values of σ when compared at the same temperature, while their values of σ are quite different when compared at temperatures corresponding to a given mean correlation time. The implications of the observed temperature dependence of the mean and the width of the correlation time distribution are discussed next.

4. Discussion

4.1. A Unified View of Dynamic Heterogeneity. In light of the deuteron NMR results, the variety of previous observations on the dynamic heterogeneity in blends can now be viewed in a unified way. Measurements of the rate of segmental motion of each species in a miscible blend of PI/PVE show two different types of dynamic heterogeneities simultaneously: the broad distribution of the dynamics of each species, and the distinct mean correlation times of individual species. Furthermore, the results suggest a unified view that interrelates these molecular level dynamics and macroscopic properties such as the broad glass transition and the thermorheological complexity of blends.

Some of the distinctive and potentially useful (or deleterious) macroscopic properties of miscible blends, particularly the anomalously broad glass transition evident in DSC[3,4] and mechanical measurements,[15] originate in a broadening of the distribution of segmental motional rates upon mixing. To control these properties, it is necessary to understand how they are related to underlying molecular motions. Therefore, spectroscopic methods have been applied to observe the dynamics of each species. In blends in which the dielectric response is dominated by one component, dielectric spectra have shown that blending can broaden the motional spectrum of an individual component.[5,14] Researchers focusing on these results have emphasized the role of broadening of the dynamics of each component in producing the broad macroscopic glass transition. However, they lacked information on the difference between the dynamics of the two components or the relationship between the broadening of the spectrum of one component to that of the other. Similar limitations apply to 2D ^{13}C NMR studies of only one component in

a miscible blend, which provide information on the spectrum of motional rates for only the labeled species.[16]

Other spectroscopic methods have provided information on particular averages of the motional spectrum. Relaxation times and line widths for distinct ^{13}C NMR lines provide information on the mean motional rate of each species in a blend and have shown that they can be well separated.[9,10] In addition, differences in the temperature dependence of the mean rate of segmental motion are evident also in the failure of time–temperature superposition in blends.[7] However, the observables in these experiments provide little information on the distribution of motional rates for each species: NMR line widths are coupled to the dynamics only at particular frequencies of motion, and dynamic mechanical spectra are intrinsically broad. Perhaps as a consequence, researchers focusing on this type of information have emphasized the role of differences in mean mobility between the two components in explaining the complex thermal and thermorheological behavior of blends.

Thus, even for the relatively simple case of miscible polymer blends, dynamic heterogeneities and their manifestations in macroscopic properties have not been completely characterized in a coherent way. The difficulties associated with resolving the dynamics of individual components have been tackled only by limited methods, and the outcomes, being incomplete, led to seemingly contradictory explanations of macroscopic phenomena.

The quantitative information on the mobilities of each component provided by 2D ^{2}H NMR is unique in allowing us to assess the importance of both the broadening of the dynamics and the difference between the mean motional rates of the individual components. These show that the difference in $\tau_{c_0}(T)$ between the two components in a 50/50 PI/PVE blend leads to a difference of approximately 10 K in their effective glass transition temperatures T_g*. However, this cannot completely explain the overall width of the DSC glass transition of this blend, which is roughly 40 K (Figure 1). The observed width of the correlation time distribution σ (Figure 6) shows that, for each component, the temperature range over which motions reach the rate correlated with the DSC glass transition is very broad for each component in the blend. In light of these results, the broad distribution of dynamics of each species plays the major role in explaining the broad glass transition in blends like PI/PVE. On the other hand, the difference in mean motional rates between the two species cannot be neglected in a quantitative description of the broad glass transition.

In relation to understanding the longer range dynamics that control melt rheology, it is useful to focus on the information 2D ^{2}H NMR provides about the mean motional rate of the two species. Previous 2D ^{2}H NMR studies of homopolymers have shown that the mean rates of the segmental motions manifested in the 2D spectra fall on the same WLF behavior as the dynamic mechanical behavior of the melt.[34,37,38] From this it has been inferred that the segmental dynamics manifested in the deuteron exchange NMR experiment are intimately related to the chain motions that propagate out through the Rouse-like and reptation-like relaxations.[37,38] Although this remains to be established for the case of miscible blends, it suggests that the distinct temperature dependencies of τ_c for PI and PVE will lead into distinct temperature dependencies of the monomeric friction for each species, $\zeta_{0,i}(T)$ for species i. Furthermore, the observation of different effective glass transition temperatures for each species is reminiscent of the description of the failure of time–temperature superposition in terms of distinct values of the glass transition temperature used in the WLF dependence of $\zeta_{0,i}(T)$ for each species.[7]

To further advance the understanding of the dynamic heterogeneity in blends, we should examine the two origins that have been hypothesized in the literature: differences in intrinsic mobility between the two components[7,9] and variations in mobility due to local compositional heterogeneity.[8,14,42] The concept of intrinsic differences in mobility between the two components cannot explain the observed broadening of the correlation time distribution for each species. Local compositional heterogeneity in the absence of differences in intrinsic mobility, however, can qualitatively explain both a difference in the mean correlation time between the two species and an increase in the width of the correlation time distribution for both species. Therefore, the effect of spatial heterogeneity must be examined[3,14,42] more closely to see if it can explain the observed behavior of both the mean and the width of the correlation time distribution for both components. To do so, we consider a simple model of compositional heterogeneity that is appropriate for the case of $\chi \simeq 0$.

4.2. Effect of Statistical Variation of Local Composition. While the mobilities of the two species in the blend differ significantly from one another, this difference is small compared to the change in their mobilities with respect to their pure states (Figure 4). This suggests that the dynamics of both species are strongly dependent on the composition of their surroundings. This is consistent with the pronounced broadening of the distribution of segmental mobility for both species (Figure 6), which suggests that their dynamics are very sensitive to variations in the local composition.

In a blend with very weak interactions ($\chi \simeq 0$), one can assume that the neighbors of a particular chain are chosen randomly. Thus, the composition of its neighbors will have some distribution about the mean composition. Local segmental dynamics of a flexible chain appear to be sensitive to the neighboring chains lying within a distance that has been estimated to be 2–7 nm.[14,42,43] Obviously, the influence of the immediate neighbors is the greatest, with the interactions decaying with distance. A primitive statistical model that takes into account only the nearest neighbors on a cubic lattice has been used to explain 2D NMR line shapes in a miscible blend and polymer–diluent systems.[16,44] As a crude yet more realistic approximation, one can assume that the dynamics of a test segment are coupled to all neighbors within a certain distance or critical radius r_c. Here, we assume that the mobility of a test segment depends only on the local composition within an imaginary sphere of radius r_c centered on the test segment. The composition of the neighbors can be approximated by a random statistical distribution. The size of the region that influences the dynamics naturally affects the distribution of local composition: as r_c decreases, the number of neighboring units within r_c decreases and the width of the distribution of the local composition increases.

To connect this distribution of composition with the distribution of motional rates, one must adopt some mapping of composition to mobility. Here we take the approach suggested by Fischer and co-workers.[14] Their model of dynamic heterogeneity in a mixture of polymers denoted by A and B is based on the following assumptions:

1. The local dynamics are taken to be sensitive to the composition within a subvolume of a given size. The volume fraction of component A in each subvolume is ϕ. The distribution of ϕ is assumed to be Gaussian with a variance $\langle \delta\phi^2 \rangle$.

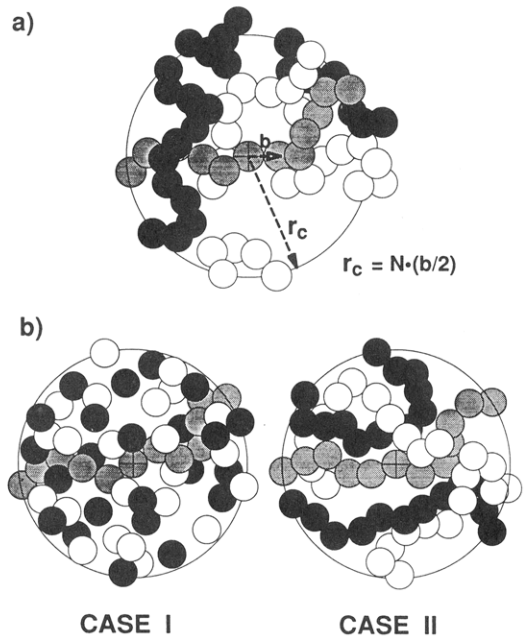

Figure 7. Schematic description of the local composition variation in a model miscible blend of chains A and B, denoted by black and white beads. The central gray chain can be either A or B, with a probability of $\tilde{\phi}$ of being A. Each subvolume of radius $r_c = N(b/2)$, where b is the size of a statistical segment, contains N^3 sites for monomer segments. (a) One possible realization of an actual subvolume, with strands of various lengths passing through it. (b) Two limiting cases: case I, a subvolume filled by independent segments; case II, a subvolume filled by independent strands of uniform length of $N^2/2$.

2. The value of ϕ in each subvolume remains constant on the time scale of the α relaxation.

3. A subvolume has a local glass transition temperature T_g^{loc} that depends only on ϕ; and the ϕ dependence of $T_g^{loc}(\phi)$ is assumed to be the same as that of the macroscopic T_g.

4. The correlation time of a subvolume $\tau(\phi,T)$ is calculated by the WLF equation, with the parameters (C_1^g, C_2^g) taken as the average of the pure components' values, and using the empirical $T_g^{loc}(\phi)$. Fischer has used this model to quantitatively describe the gradual broadening of the α relaxation spectra by using $\langle\delta\phi^2\rangle$ as a temperature-dependent fitting parameter.[14] The temperature dependence of $\langle\delta\phi^2\rangle(T)$ was interpreted as arising from the temperature dependence of the subvolume size. The radius of the subvolume was estimated to be approximately 7 nm at T_g + 20 K and decreases with temperature.[14] The subvolume was interpreted as the cooperatively relaxing unit.[45]

Our goal is to see if this physical picture is capable of describing the observed correlation time distribution for both components simultaneously. Although we adopt the mapping of local composition to mobility introduced by Fischer and co-workers, our calculation differs from theirs in a few respects. In Fischer's model, the sample is divided into small subvolumes and all segments in a subvolume have the same mobility. Here, the subvolumes are constructed around every test segment and the mobility of that test segment is obtained from the composition of its subvolume. Instead of using $\langle\delta\phi^2\rangle$ as a temperature-dependent fitting parameter and using it to estimate the size of subvolumes, we start with a simple statistical model to estimate $\langle\delta\phi^2\rangle$ as a function of the subvolume size. The temperature dependence of the subvolume size is neglected in our calculations. We assume that the mixing is random at a molecular level, which is consistent with the observation that PI/PVE is miscible without any specific interaction between the species.[21] We also neglect the effects of slight densification (ca. 0.1%) and any difference in the packing efficiency of the blend compared to the homopolymers.[18,19] The correlation time distributions of the components in a blend are then calculated by following the assumptions introduced by Fischer and co-workers.[14]

In this model, the subvolumes around each test segment are constructed as illustrated in Figure 7. In a subvolume with diameter Nb, there are N^3 sites for segments, each with a volume of $4/3\pi(b/2)^3$, where b is the size of the statistical segment. A given subvolume is identified as an A or a B subvolume depending upon the type of test segment at the center of the subvolume. The test chain that contains this central segment is assumed to occupy $N^2/2$ sites, i.e., the mean number occupied by two random walks that begin at the origin and end a distance $r_c = Nb/2$ from it. The remaining N^3–$N^2/2$ sites are filled by either A or B randomly. Thus, the composition in the subvolume is biased toward that of the test chain due simply to connectivity of segments along the chain.[3,16,44] When the volume fraction of A for the macroscopic sample is $\tilde{\phi}$, the mean composition of subvolumes centered on an A segment is

$$\langle\phi\rangle_A = \frac{1}{2N} + \left(1 - \frac{1}{2N}\right)\tilde{\phi} \tag{3}$$

and the mean volume fraction of A in the subvolumes centered on a B segment is

$$\langle\phi\rangle_B = \left(1 - \frac{1}{2N}\right)\tilde{\phi} \tag{4}$$

where the subscript (A or B) denotes the identity of the test segment for the subvolumes included in the average.

The width of the distribution of ϕ depends on the number of independent units that participate in filling the $N^3 - N^2$ empty sites. The estimation of the composition variation is particularly simple when the empty sites are filled by independent units of equal size. In selecting this fixed size, there are two extreme cases, as illustrated in Figure 7b; the independent unit is taken in one case to be a single segment (case I) and in the other a strand of N^2 segments, like the test chain (case II). The composition variation $\langle\delta\phi^2\rangle$ estimated from case I denoted by $\sigma^2_{\phi,1}$ gives a lower bound on $\langle\delta\phi^2\rangle$, whereas the composition variation from case II ($\sigma^2_{\phi,N}$) sets a practical upper bound. The variance of the volume fraction is the same for both the A and B subvolumes and is obtained by applying the statistics of Bernoulli Trials. In the case that $N^3 - N^2$ remaining sites are filled by independent segments, the variance of ϕ is

$$\sigma^2_{\phi,1} = \frac{\tilde{\phi}(1-\tilde{\phi})}{N^3 - N^2/2} \tag{5}$$

and in the case that sites are filled by $N - 1$ independent strands of N^2 segments, the variance is

$$\sigma^2_{\phi,N} = \frac{\tilde{\phi}(1-\tilde{\phi})}{2N - 1} \tag{6}$$

where the subscript 1 or N denotes filling by single segments or strands of N segments. The composition distribution of each subvolume $P_i(\phi)$ is further approximated as Gaussian with the mean and the variance of

composition obtained above, *i.e.*

$$P_{i,n}(\phi) = \frac{1}{(2\pi\sigma^2_{\phi,n})^{1/2}} \exp[-(\phi - \langle\phi\rangle_i)^2/2\sigma^2_{\phi,n}] \quad (7)$$

where $P_{i,n}(\phi)$ is the probability that a subvolume has a particular composition ϕ given that the test segment is type i (A or B) and the mode of "filling" is designated by n (1 or N).

Under the assumptions introduced by Fischer and coworkers, the composition of a subvolume, ϕ, is directly mapped onto the correlation time for segmental motion of all chains in that subvolume, $\tau(\phi,T;T_g^{loc}(\phi))$:

$$\log\{\tau(\phi,T;T_g^{loc}(\phi))\} = \log \tau_g - \frac{C_1^g(T - T_g^{loc}(\phi))}{C_2^g + (T - T_g^{loc}(\phi))} \quad (8)$$

where τ_g is the correlation time for the motion at $T = T_g^{loc}$. Here, we use the empirical value $\tau_g = 0.32$ s as described earlier. In our calculation, we take τ to be that of the test segment, rather than that of all segments in the subvolume. Although $\tau(\phi,T;T_g^{loc}(\phi))$ is taken to be the same for both species in a blend, the mean correlation times of the two species can differ significantly due to the bias in the composition distribution toward that of the test chain (eqs 3 and 4). The width of the distribution of correlation times for the two components can also differ, due to the nonlinear dependence of τ on ϕ through T_g. We let A denote the higher T_g component and B the lower T_g component, corresponding in our experiments to PVE and PI, respectively. The composition-dependent glass transition temperature ($T_g^{loc}(\phi)$) is approximated by the quadratic fit of the DSC T_g of PI/PVE blends reported by Roovers and Toporowski.[7]

We calculate the correlation time distribution of A and B subvolumes directly from the above composition distribution. The log mean correlation times ($\log \tau_{i,n}$) and the distribution widths ($\sigma_{i,n}$) are subsequently calculated as averages over the subvolumes:

$$\log \tau_{i,n} = \int_0^1 [\log\{\tau(\phi,T;T_g^{log}(\phi))\}] P_{i,n}(\phi)\, d\phi \quad (9)$$

and

$$\sigma_{i,n}{}^2 = \int_0^1 [\log\{\tau(\phi,T;T_g^{loc}(\phi))\} - \log \tau_{i,n}]^2 P_{i,n}(\phi)\, d\phi \quad (10)$$

where i is A and B according to the identity of the test segment and n is 1 or N specifying case I or II.

The behaviors of the $\log \tau_i$'s and σ_i's agree qualitatively with the experimental observations, for both cases I and II. At all temperatures, the mean correlation times of A and B are biased toward that in their pure state. The differences between the mean correlation times and the distribution widths of both A and B chains increase with decreasing temperature. However, neither of the two cases can capture the relative magnitude of the difference in mean correlation times and the width of the distribution.

In case I the width of the composition distribution decreases strongly with subvolume size ($\sigma^2_{\phi,1} \sim N^{-3}$, eq 5), so even a very small size ($N \approx 3$) cannot capture the observed width of the distribution of motional rates. Further, when the subvolume is this small, the bias in composition toward that of the test chain is large and produces a bimodal distribution of motional rates overall. Finally, the A subvolumes (rich in the high-T_g component) have a significantly broader distribution of motional rates than the B subvolumes due to the increasing sensitivity of T_g to the volume fraction of the high-T_g component ϕ as $\phi \to 1$. Thus, case I cannot describe the observed distribution of motional rates.

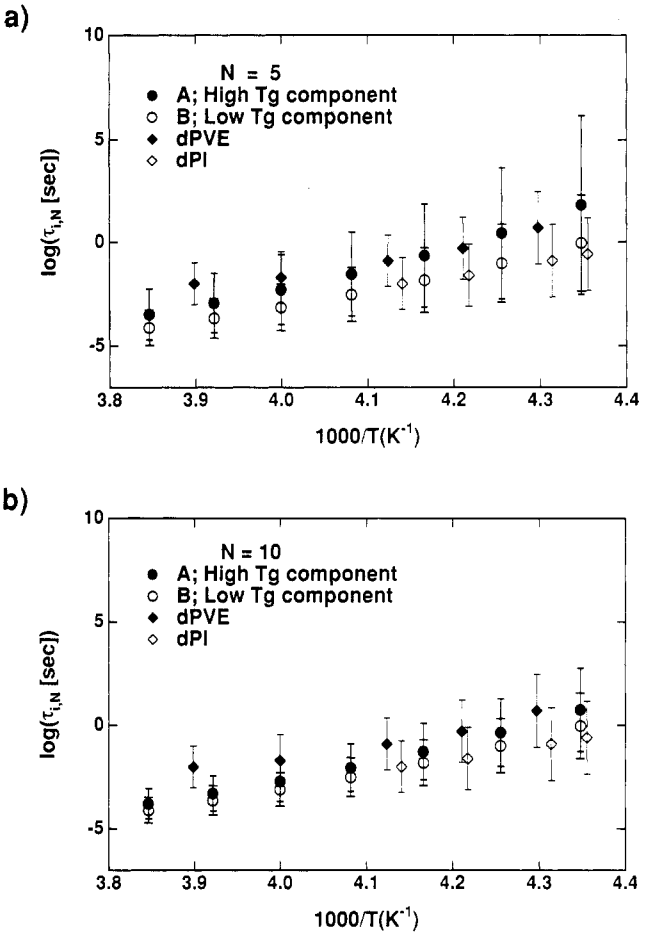

Figure 8. Mean and width of the correlation time distribution ($\log \tau_{i,N}$, $\sigma_{i,N}$) that are calculated for case II, where i is the identity of the test chain A and B. (a) For a subvolume size of $N = 5$, the difference in the mean correlation times $\tau_{c_0,A} - \tau_{c_0,B}$ is comparable to the experiments. (b) For $N = 10$, the distribution widths σ_A and σ_B are comparable to the experimental values.

For case II, since the subvolumes are filled by independent strands of N^2 segments, the width of the composition distribution for a given N is much wider than that in case I. The subvolume size that gives $\sigma^2_{\phi,N}$ in accord with the experimental results is $N \simeq 10$ (Figure 8b). For this size, the segments of the test chain constitute a minor fraction of all the segments in the subvolume, and the difference between the mean composition and the associated motional rate for the A and B subvolumes is relatively small. As a result, the composition distributions of A and B subvolumes are strongly overlapped and the overall correlation time distribution becomes unimodal, in accord with experiment. In addition, for $N \geq 10$, $\sigma_{A,N}$ and $\sigma_{B,N}$ become similar to each other, which is also in agreement with experiment. However, for a subvolume size that captures the approximate magnitudes of σ_A and σ_B and their relative magnitude, the difference between the mean correlation times is much smaller than is observed experimentally (see Figure 8b). To capture the observed difference between the mean correlation times, the size of the subvolume must be reduced to $N \simeq 5$ (Figure 8a). This results in an increase in the distribution widths and an increase in $\sigma_{A,N}$ relative to $\sigma_{B,N}$ for the reasons discussed earlier in relation to case I.

Thus, the present physical picture cannot capture simultaneously the separation in the mean correlation times *and* the two distribution widths for any choice of

the subvolume size. When the distribution widths of the correlation times are comparable to the experimental values, the difference in the mean correlation times is significantly smaller than what is found experimentally. This is also true for any case intermediate between cases I and II. Therefore, we infer that compositional variation alone cannot explain the observed effects of blending on the correlation time distributions of the two components. Composition variations can explain the increase in the width of the distribution of motional rates. However, if the subvolume size captures the observed σ_A and σ_B, it only explains a small fraction of the observed difference between the mean motional rates of A and B. The remaining difference in the mean correlation times can be attributed to intrinsic mobility differences between the two components.

5. Conclusions

We have presented quantitative measurements of the rates of segmental rearrangement of each species in a PI/PVE miscible blend. By gaining direct information on the mean and distribution of motional rates as a function of temperature, we have been able to unify many previous observations of dynamic heterogeneity in blends. In particular, the 2D ^2H NMR results show that previous observations of either distinct dynamics of each species (*e.g.*, by ^{13}C NMR and failure of time–temperature superposition) or broadening of the dynamics of one or both species (*e.g.*, by dielectric or DSC measurements) can be reconciled into a unified picture. Further, two possible origins of the dynamic heterogeneities are examined by comparing the experimental results to a simple model calculation that takes into account the effect of composition variations in a blend. When the mobility of each chain is controlled solely by local composition regardless of the identity of the chain, the observed behavior of the mean and the width of the correlation time distributions could not be explained simultaneously. This suggests that the observed dynamic heterogeneities can only be explained by including two distinct contributions: the local composition variation in the blend *and* the intrinsic difference in chain mobilities.

The results show how significant dynamic heterogeneity arises even in a single-phase polymer blend when the pure components have widely separated glass transitions and have sufficiently weak interactions that statistical composition variation is significant. These conditions lead to separate effective glass transitions for the two components, which contributes to the broad glass transition and may underlie the failure of time–temperature superposition in the plateau and terminal regimes. In addition, these conditions lead to a broad distribution of local motional rates for each species, which can dominate the broad calorimetric and mechanical glass transition.

To gain further information on the effect of local composition on the dynamics of PI and PVE, 2D ^2H exchange NMR measurements are underway on other blend compositions. To determine the relationship between the local segmental dynamics investigated here and the macromolecular relaxation processes that control the viscoelasticity of molten miscible blends, we are conducting rheooptical studies that combine conventional dynamic mechanical measurements with dynamic birefringence[17] and IR dichroism. This approach should also be extended to blends that are miscible due to attractive interactions to examine the effects of the resulting bias in the composition of neighboring chains and of possible coupling between the motions of the two components.

Acknowledgment. We gratefully acknowledge the support of the National Science Foundation Presidential Young Investigator Award (J.A.K.), Chevron, and the Caltech Consortium in Chemistry and Chemical Engineering: E. I. du Pont de Nemours and Co., Inc., and Eastman Kodak Co.

References and Notes

(1) *Multicomponent Polymer Systems*; Miles, I. S., Rostami, S., Eds.; Polymer Science & Technology Series; Longman Scientific & Technical: Harlow, U.K., 1992.
(2) *Polymer–Polymer Miscibility*; Olabisi, O., Robeson, L. M., Shaw, M. T., Eds.; Academic Press: San Diego, 1979.
(3) Lau, S.; Pathak, J.; Wunderlich, B. *Macromolecules* **1982**, *15*, 1278.
(4) Lin, J.-L.; Roe, R.-J. *Polymer* **1988**, *29*, 1227.
(5) Zetsche, A.; Kremer, F.; Jung, W.; Schulze, H. *Polymer* **1990**, *31*, 1883.
(6) Trask, C. A.; Roland, C. M. *Macromolecules* **1989**, *22*, 256.
(7) Roovers, J.; Toporowski, P. M. *Macromolecules* **1992**, *25*, 3454.
(8) Colby, R. H. *Polymer* **1989**, *20*, 1275.
(9) Miller, J. B.; McGrath, K. J.; Roland, C. M.; Trask, C. A.; Garroway, A. N. *Macromolecules* **1990**, *23*, 4543.
(10) Le Menestrel, C.; Kenwright, A. M.; Sergot, P.; Laupretre, F.; Monnerie, L. *Macromolecules* **1992**, *25*, 3020.
(11) Zawada, J. A.; Ylitalo, C. M.; Fuller, G. G.; Colby, R. H.; Long, T. E. *Macromolecules* **1992**, *25*, 2896.
(12) (a) Composto, R. J.; Kramer, E. J.; White, D. M. *Macromolecules* **1988**, *21*, 2580. (b) Composto, R. J.; Kramer, E. J.; White, D. M. *Polymer* **1990**, *31*, 2320.
(13) Zhao, Y.; Jasse, B.; Monnerie, L. *Polymer* **1989**, *30*, 1643.
(14) Fischer, E. W.; Zetsche, A. *Polym. Prepr. (Am. Chem. Soc., Div. Polym. Chem.)* **1992**, 78.
(15) Roland, C. M.; Ngai, K. L. *Macromolecules* **1991**, *24*, 2261.
(16) Chin, Y. H.; Zhang, C.; Wang, P.; Inglefield, P. T.; Jones, A. A.; Kambour, R. P.; Bendler, J. T.; White, D. M. *Macromolecules* **1992**, *25*, 3031.
(17) Arendt, B. H.; Kannan, R. M.; Zewail, M.; Kornfield, J. A.; Smith, S. D., submitted to *Rheol. Acta*.
(18) Tomlin, D. W.; Roland, C. M. *Macromolecules* **1992**, *25*, 2994.
(19) Roland, C. M.; Miller, J. B.; McGrath, K. J., submitted to *Macromolecules*.
(20) Roland, C. M. *Macromolecules* **1987**, *20*, 2557.
(21) Roland, C. M. *J. Polym. Sci., Polym. Phys. Ed.* **1988**, *26*, 839.
(22) Bates, F. S.; Rosadale, J. H.; Bair, H. E.; Russell, T. P. *Macromolecules* **1989**, *22*, 2557.
(23) Sakurai, S.; Jinnai, H.; Hasegawa, H.; Hashimoto, T.; Han, C. C. *Macromolecules* **1991**, *24*, 4839.
(24) This is in contradiction to recent two-dimensional heteronuclear correlation NMR studies where a nonrandom packing between PI and PVE is suggested (Mirau, P. MRS Meeting, Boston, 1992). However, the NMR result and its interpretation are not yet fully confirmed.
(25) Roovers, J.; Wang, F., submitted to *J. Non-Cryst. Solids*.
(26) Carella, J. M.; Graessley, W. W.; Fetters, L. J. *Macromolecules* **1984**, *17*, 2775.
(27) Ferry, J. D. *Viscoelastic Properties of Polymers*; John Wiley & Sons: New York, 1970.
(28) Further, previous studies show that crystallization is inhibited severely in a miscible blend: the crystalline fraction is less than 30% even for pure *cis*-1,4-polyisoprene and becomes negligible in blends with more than 25% 1,2-polybutadiene fraction.[20] As expected for a completely amorphous sample, neither symmetric jump motions nor effectively rigid segments characteristic of a crystalline fraction are evident in our experimental NMR spectra.
(29) Schmidt, C.; Wefing, S.; Blümich, B.; Spiess, H. W. *Chem. Phys. Lett.* **1986**, *130*, 84.
(30) Schmidt, C.; Blümich, B.; Spiess, H. W. *J. Magn. Reson.* **1988**, *79*, 269.
(31) Spiess, H. W. In *NMR—Basic Principles and Progress*; Diehl, P., Fluck, E., Kosfeld, R., Eds.; Springer-Verlag: New York, 1978; Vol. 15.
(32) Schaefer, D. Ph.D. Thesis, University of Mainz, Mainz, Germany, 1992. This pulse sequence is a modification of the previous four-pulse sequence[29] to eliminate the need for extrapolation in the t_1 dimension to obtain $t_1 = 0$ data.
(33) Since the range of times t_1 and t_2 is short ($\leq 2 \times 10^{-4}$ s) compared to the characteristic time for reorientation of C–^2H bonds in a polymer near T_g ($\tau_c \geq 10^{-3}$ s), we can neglect reorientation during t_1 and t_2.[34]

(34) Kaufmann, S.; Wefing, S.; Schaefer, D.; Spiess, H. W. *J. Chem. Phys.* **1990**, *93*, 197.
(35) The variation from the set temperature is less than ±0.5 K. However, the Bruker thermocouple reading of the absolute sample temperature is frequently incorrect. To overcome this problem, an additional thermocouple is built in near the sample. The temperature measurement is further tested by placing another thermocouple at the center of the sample tube and comparing the readings from all three thermocouples. The reading from the new built-in thermocouple turned out to be more reliable, probably due to the smaller distance from the sample than the Bruker one. In this paper, the data are reported in reference to this temperature. It is also noticed that the Bruker thermocouple reading is always higher than the test thermocouple reading by about 3–5 °C below 0 °C, consistent with the apparent temperature offset between the previous 2D ^{2}H NMR results for PI[36] and our own (Figure 5).
(36) Schaefer, D.; Spiess, H. W. *J. Chem. Phys.* **1992**, *97*, 7944.
(37) Schaefer, D.; Spiess, H. W.; Suter, U. W.; Fleming, W. W. *Macromolecules* **1990**, *23*, 3431.
(38) Pschorn, U.; Rössler, E.; Sillescu, H.; Kaufmann, S.; Schaefer, D.; Spiess, H. W. *Macromolecules* **1991**, *24*, 398.
(39) Wefing, S.; Kaufmann, S.; Spiess, H. W. *J. Chem. Phys.* **1988**, *89*, 1234.
(40) Schmidt-Rohr, K.; Spiess, H. W. *Phys. Rev. Lett.* **1991**, *66*, 3020.
(41) In previous 2D ^{2}H NMR, light scattering, and mechanical measurements, mean correlation times of 10^1–10^3 s were reported at the DSC glass transition.[34,36–38,46,47] This is about 2 orders of magnitude slower than our observations, and this difference should be examined further by using a consistent definition of the DSC T_g and by controlling the absolute temperatures more accurately.[35] The relationship between the NMR correlation times and macroscopic relaxation times has not been clearly established.
(42) Schmidt-Rohr, K.; Clauss, J.; Spiess, H. W. *Macromolecules* **1992**, *25*, 3273.
(43) Donth, E. *J. Non-Cryst. Solids* **1982**, *53*, 325.
(44) Cauley, B. J.; Cipriani, C.; Ellis, K.; Roy, A. K.; Jones, A. A.; Inglefield, P. T.; McKinley, B. J.; Kambour, R. P. *Macromolecules* **1991**, *24*, 403.
(45) Adam, G.; Gibbs, J. H. *J. Chem. Phys.* **1965**, *76*, 139.
(46) Lee, H.; Jamieson, A. M.; Simha, R. *Macromolecules* **1979**, *12*, 329.
(47) Angel, C. A. *J. Non-Cryst. Solids* **1991**, *131–133*, 13.